Velocity and Pressure Profiles for Newtonian Creeping Flow in Regular Packed Beds of Spheres

L. J. SNYDER and W. E. STEWART

University of Wisconsin, Madison, Wisconsin

A theoretical analysis is made of Newtonian creeping flow through dense cubic and simple cubic beds of spheres. Velocity and pressure profiles are obtained in equation form by Galerkin's error-distribution method. The profiles satisfy the conservation equations approximately, and the boundary conditions and symmetry conditions exactly. The calculated friction factors are within 5% of experimental values for both packing arrangements.

Flows of fluids through packed beds are important in various chemical engineering fields. Many industrial operations use packed beds, and pressure drop relationships are required for their design. In addition, detailed velocity profiles are needed for analytical investigations of heat or mass transfer in such systems. The latter consideration motivated the study reported here.

Satisfactory empirical correlations of pressure drop are available for various packed-bed systems, including regular packed beds of spheres (*1*). Such correlations have been based largely on experimental data, although simple theoretical models sometimes have been included. One such model considered a packed bed as a network of irregular ducts (*2, 3*); another considered a packed bed as a collection of submerged objects (*4*). None of these correlations can be used to calculate velocity profiles; however, they do provide useful tests of the profiles reported here.

Velocity profiles in packed beds of spheres recently have been calculated on the basis of a "free surface" model (*5*). The pressure drop thus predicted agrees reasonably well with experimental data. However, the calculated velocity profiles must differ significantly from the actual velocity profiles in a packed bed, since the free surface model assumes that none of the spheres are touching each other.

Velocity profiles in regular arrays of spheres have been calculated approximately by Uchida (*6*), Brenner (*7*), and Hasimoto (*8*). Uchida and Brenner included packed (dense) arrays, whereas Hasimoto considered only dilute arrays. The results for packed arrays are not very accurate, due to the use of too few terms in the series solutions. Extensive calculations would be necessary to continue those series to the level of accuracy attained here.

This paper gives a new analysis of the pressure and velocity profiles in dense cubic and simple cubic packed beds. The profiles are expanded in terms of new trial functions which satisfy the boundary conditions and periodicity conditions. The coefficients in the expansions are computed by Galerkin's method. The pressure drop relations obtained agree well with experimental data (*1*) for both packing arrangements.

L. J. Snyder is with Esso Production Research Company, Houston, Texas.

STATEMENT OF THE PROBLEM

The system chosen for the major part of this study is a bed of spheres in a dense cubic packing arrangement as shown in Figure 1. The sphere centers are in the planes

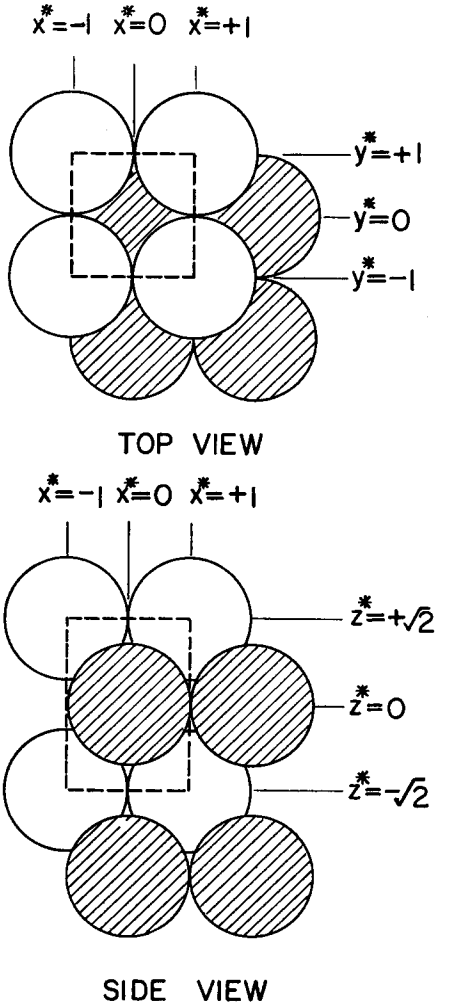

Fig. 1. Dense cubic packing arrangement.

$z/R = 0, \pm\sqrt{2}, \pm 2\sqrt{2}, \ldots$, and form a square lattice in each such plane. The unit cell enclosed by the dotted lines contains the sphere centered at 0, 0, 0, and portions of the eight adjacent spheres. This packing arrangement has a void fraction near that of tight random packing and provides a very stable system for experimental work (*1*).

Consider the steady state creeping flow of a constant-property Newtonian fluid through the void space of the packed bed. The main flow is in the positive z direction. In creeping flow the inertial terms in the Navier-Stokes equation are negligible. Wall effects, entrance effects, and end effects are ignored. The velocity is, therefore, taken as a periodic function of x, y, and z, and the pressure as a periodic function of x, y, and z plus a linear function of z. Therefore, it is only necessary to calculate the profiles in one unit cell of the packing.

It is convenient to adopt the dimensionless variables

$$x^* = x/R;\ y^* = y/R;\ z^* = z/R \tag{1}$$

$$\mathbf{v}^* = \mathbf{v}\mu/(\mathcal{P}_0 - \mathcal{P}_L)R \tag{2}$$

$$\mathcal{P}^* = (\mathcal{P} - \mathcal{P}_0)/(\mathcal{P}_L - \mathcal{P}_0) \tag{3}$$

in which R is the radius of the spheres and $\mathcal{P}_0$ and $\mathcal{P}_L$ are the values of the function $\mathcal{P} = p + \rho gh$ at the planes $z^* = -\sqrt{2}$ and $z^* = \sqrt{2}$. The dimensional quantities x, y, z, R, $\mathbf{v}$, μ, $\mathcal{P}_0$, and $\mathcal{P}_L$ will not appear again until the end of the analysis.

The velocity and pressure profiles in the void space of the packed bed are governed by the equation of continuity

$$\frac{\partial v_x^*}{\partial x^*} + \frac{\partial v_y^*}{\partial y^*} + \frac{\partial v_z^*}{\partial z^*} = 0 \tag{4}$$

the x component of the equation of motion

$$\frac{\partial \mathcal{P}^*}{\partial x^*} + \left[\frac{\partial^2 v_x^*}{\partial x^{*2}} + \frac{\partial^2 v_x^*}{\partial y^{*2}} + \frac{\partial^2 v_x^*}{\partial z^{*2}}\right] = 0 \tag{5}$$

the y component of the equation of motion

$$\frac{\partial \mathcal{P}^*}{\partial y^*} + \left[\frac{\partial^2 v_y^*}{\partial x^{*2}} + \frac{\partial^2 v_y^*}{\partial y^{*2}} + \frac{\partial^2 v_y^*}{\partial z^{*2}}\right] = 0 \tag{6}$$

and the z component of the equation of motion

$$\frac{\partial \mathcal{P}^*}{\partial z^*} + \left[\frac{\partial^2 v_z^*}{\partial x^{*2}} + \frac{\partial^2 v_z^*}{\partial y^{*2}} + \frac{\partial^2 v_z^*}{\partial z^{*2}}\right] = 0 \tag{7}$$

Note that the differential equations in dimensionless form do not depend on the sphere radius R, the characteristic pressure drop $\mathcal{P}_0 - \mathcal{P}_L$, or the viscosity of the fluid. The boundary conditions on pressure are

$$\mathcal{P}^* = 0 \text{ at } z^* = -\sqrt{2}$$
$$\mathcal{P}^* = 1 \text{ at } z^* = +\sqrt{2} \tag{8}$$

The no-slip condition requires that

$$\mathbf{v}^* = 0 \tag{9}$$

on the sphere surfaces. Additional boundary conditions on the velocity components and their first derivatives are

at $x^* = 0, \pm 1$

$$v_x^* = \frac{\partial v_y^*}{\partial x^*} = \frac{\partial v_z^*}{\partial x^*} = 0 \tag{10}$$

at $y^* = 0, \pm 1$

$$v_y^* = \frac{\partial v_x^*}{\partial y^*} = \frac{\partial v_z^*}{\partial y^*} = 0 \tag{11}$$

and at $z^* = 0, \pm\sqrt{2}$

$$v_x^* = v_y^* = \frac{\partial v_z^*}{\partial z^*} = 0 \tag{12}$$

The last three equations follow from the symmetry and periodicity of the fully developed flow; they were found in the same way by Brenner (*7*). These boundary conditions and differential equations admit only one solution, as shown by Johnson (*9*); therefore, the flow problem is completely formulated.

Each of the spheres must have the same velocities and pressure gradients around it. Furthermore, the streamlines must be symmetric in the z direction. It follows that the symmetries with respect to the coordinate axes are as follows: v_x^* is symmetric about the plane $y^* = 0$ and antisymmetric about the planes $x^* = 0$ and $z^* = 0$; v_y^* is symmetric about the plane $x^* = 0$, and antisymmetric about the planes $y^* = 0$ and $z^* = 0$; v_z^* is symmetric about the planes $x^* = 0$, $y^* = 0$, and $z^* = 0$; and $\mathcal{P}_{per}^*$, the periodic portion of $\mathcal{P}^*$, is symmetric about the planes $x^* = 0$ and $y^* = 0$, and antisymmetric about the plane $z^* = 0$. From the same considerations one obtains the relationships

$$\begin{aligned}\mathbf{v}^*(x^*, y^*, z^*) &= \mathbf{v}^*(-x^*, -y^*, -z^*)\\ &= \mathbf{v}^*(x^*, y^*, z^* + 2\sqrt{2})\\ &= \mathbf{v}^*(1-x^*, 1-y^*, \sqrt{2}-z^*)\\ &= \mathbf{v}^*(1+x^*, 1+y^*, \sqrt{2}+z^*)\end{aligned} \tag{13}$$

$$\begin{aligned}\mathcal{P}_{per}^*(x^*, y^*, z^*) &= \mathcal{P}_{per}^*(x^*, y^*, z^* + 2\sqrt{2})\\ &= \mathcal{P}_{per}^*(1+x^*, 1+y^*, \sqrt{2}+z^*)\end{aligned} \tag{14}$$

and

$$\begin{aligned}\mathcal{P}_{per}^*(x^*, y^*, z^*) &= -\mathcal{P}_{per}^*(-x^*, -y^*, -z^*)\\ &= -\mathcal{P}_{per}^*(1-x^*, 1-y^*, \sqrt{2}-z^*)\end{aligned} \tag{15}$$

between flow conditions at different points in the packed bed.

An interchange of the x^* and y^* coordinates in the differential equations and boundary conditions gives an identical set of equations; therefore, the velocity and pressure profiles must be unchanged by an interchange of the x^* and y^* axes. This requires that

$$v_x^*(x^*, y^*, z^*) = v_y^*(y^*, x^*, z^*) \tag{16}$$

$$v_z^*(x^*, y^*, z^*) = v_z^*(y^*, x^*, z^*) \tag{17}$$

and

$$\mathcal{P}^*(x^*, y^*, z^*) = \mathcal{P}^*(y^*, x^*, z^*) \tag{18}$$

These relations, along with Equations (13) to (15), are corollaries of the problem statement in Equations (4) to (12).

It appears doubtful at this time that an analytical solution can be obtained. Approximate solutions are obtainable, however, by trial function methods or finite-difference calculations. Trial function methods have the advantage of being able to satisfy boundary conditions and symmetry properties exactly. Finite-difference calculations would have difficulty with the curved boundaries. From the results of earlier studies (*10*), it was decided to obtain an approximate solution from a set of trial functions by using Galerkin's method to evaluate the unknown parameters.

DESCRIPTION OF THE TRIAL FUNCTIONS

The solution of problems in transport phenomena by Galerkin's method has been discussed in detail previously (*10, 11*). Briefly, one must first choose a set of trial functions containing adjustable parameters. For one to use an "interior" method, as is done in this work, the trial functions must satisfy the boundary conditions of the

problem. The trial solution, here taken as an arbitrary linear combination of trial functions, is substituted into each of the differential equations and may fail to satisfy the k^{th} equation locally by some amount, ϵ_{Tk}. This interior error ϵ_{Tk} is then made orthogonal to a suitable group of the trial functions over the domain of the problem. This provides a system of equations for the parameters in the trial solution. The determination of the parameters completes the approximate solution.

The selection of a set of trial functions for this problem is difficult. A complete set of functions which is appropriately periodic in the x, y, and z directions, which satisfies the boundary conditions of the problem, and which has the necessary symmetry properties, is desired. Here, as in most applications, completeness in a least squares (L_2) sense (*12*) is desired. It would also be advantageous for the trial functions to satisfy some of the differential equations. An attempt was made to find a velocity trial solution which satisfied all the velocity boundary conditions and the equation of continuity, but without success.

The trial solutions finally selected for the dense cubic packing are as follows:

$$v_z^* = \sum_{i=1}^{N} C_{zi}\,\chi \cos \alpha_i\,\pi x^* \cos \beta_i\,\pi y^* \cos \gamma_i \frac{\pi z^*}{\sqrt{2}} = \sum_{i=1}^{N} C_{zi}\chi\,\phi_{zi} \tag{19}$$

$$v_x^* = \sum_{i=1}^{N} C_{xi}\chi \sin\,(\alpha_i + 1)\,\pi x^* \cos \beta_i\,\pi y^* \cdot \sin\,(\gamma_i + 1)\frac{\pi z^*}{\sqrt{2}} = \sum_{i=1}^{N} C_{xi}\chi\,\phi_{xi} \tag{20}$$

$$v_y^* = \sum_{i=1}^{N} C_{yi}\chi \cos \alpha_i\,\pi x^* \sin\,(\beta_i + 1)\,\pi y^* \cdot \sin\,(\gamma_i + 1)\frac{\pi z^*}{\sqrt{2}} = \sum_{i=1}^{N} C_{yi}\chi\,\phi_{yi} \tag{21}$$

and

$$\mathcal{P}^* = \frac{(z^* + \sqrt{2})}{2\sqrt{2}} + \sum_{i=1}^{N} C_{Pi} \cos \alpha_i'\,\pi x^* \cos \beta_i'\,\pi y^* \cdot \sin\,(\gamma_i' + 1)\frac{\pi z^*}{\sqrt{2}} = \frac{(z^* + \sqrt{2})}{2\sqrt{2}} + \sum_{i=1}^{N} C_{Pi}\phi_{Pi} \tag{22}$$

Here, the C_{xi}, C_{xi}, C_{yi}, and C_{Pi} are adjustable parameters (coefficients) which must be determined to complete the approximate solution.

The function χ is included in the velocity profiles to satisfy the no-slip condition at the sphere surfaces. This function is required to be zero on the sphere surfaces, to be positive in the void space of the bed, and to have the symmetry properties of v_z^*. A function of the form

$$\chi = \prod_{l=1}^{\infty} G_l \tag{23}$$

where G_l is a positive function of d_l, the distance from the l^{th} sphere, meets these requirements. This type of function is meaningful only if $G_l \to 1.0$ as d_l increases, and for ease of calculation it is desirable that this asymptote be approached rather quickly.

The first χ function tried was

$$\chi_I = \prod_{l=1}^{\infty} \left[1.0 - \frac{1.0}{[(x^* - x_l^*)^2 + (y^* - y_l^*)^2 + (z^* - z_l^*)^2]^{16}} \right] \tag{24}$$

where x_l^*, y_l^*, and z_l^* are the coordinates of the center of the l^{th} sphere. Only the fourteen closest spheres need be considered to calculate values of this function within one part in 10^8. However, this function has a very blunt shape, which makes the trial solutions unrealistic unless N is quite large.

The approximate solutions presented here use the function

$$\chi_{II} = \prod_{l=1}^{\infty} \left[1.0 - \frac{1.0}{\sqrt{[x^* - x_l^*]^2 + [y^* - y_l^*]^2 + [z^* - z_l^*]^2} + 0.001([x^* - x_l^*]^2 + [y^* - y_l^*]^2 + [z^* - z_l^*]^2 - 1.0)^{16}} \right] \tag{25}$$

which has a much smoother shape. In the immediate neighborhood of a particular sphere, χ_{II} is proportional to the distance from that sphere. One must consider the nearest eighteen spheres to calculate point values of χ_{II} within one part in 10^8. A computer program written in Fortran is available (*13*) to calculate χ_{II} and its derivatives.

The trigonometric indices α_i, β_i, γ_i, α_i', β_i', and γ_i' in Equations (19) to (22) are positive integers which may be varied independently within the restrictions

$$\alpha_i + \beta_i + \gamma_i = \text{an even number} \tag{26}$$

and

$$\alpha_i' + \beta_i' + \gamma_i' = \text{an odd number} \tag{27}$$

These restrictions are necessary for the trial functions to satisfy Equations (13), (14), and (15). It was not initially understood that Equations (26) and (27) were needed, and the first trial solutions used $\alpha_i = \alpha_i'$, $\beta_i = \beta_i'$, and $\gamma_i = \gamma_i'$ with no restrictions on their sums. The approximate solutions obtained by Galerkin's method discarded all the terms which violated Equation (26) or (27).

The approximate solution will satisfy Equations (16), (17), and (18) only if certain parameters are equal. The first approximate solutions were obtained with no restriction on the parameters. In every case the parameter values obtained by Galerkin's method satisfied these requirements. In later solutions, Equations (16), (17), and (18) were used to eliminate duplicate parameters and conserve computer storage space.

The set of trial functions defined by Equations (19), (20), (21), (22), (25), (26), and (27) satisfies all the boundary conditions and symmetry properties of the problem statement. The various ϕ_i are from complete sets of functions; therefore, as the number of terms in the trial function is increased, the true solution can be approximated as accurately as desired. However, with several independent indices there is some question about the order in which terms should be added. The most effective method found was to select terms with the lowest values of $(\alpha_i^2 + \beta_i^2 + \gamma_i^2)$ or $(\alpha_i'^2 + \beta_i'^2 + \gamma_i'^2)$ first.

USE OF GALERKIN'S METHOD

An approximate solution may be obtained by using Galerkin's method to evaluate the parameters C_{xi}, C_{yi}, C_{zi}, and C_{Pi}. The trial solutions are substituted into the differential equations of the system [Equations (4), (5), (6), and (7)]. The amount by which these functions fail to satisfy each of the differential equations (the interior error) is a function of position and of the parameters. A

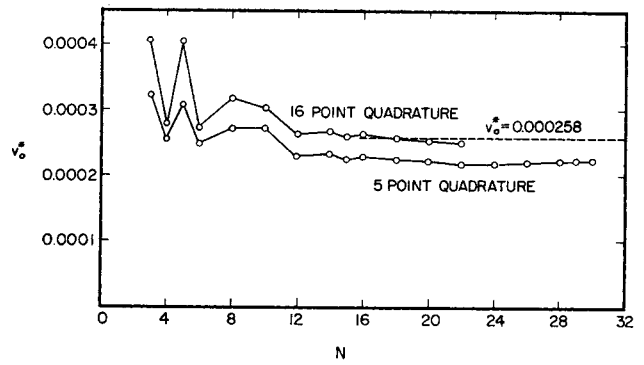

Fig. 2. Superficial velocity predicted by the approximate solutions (dense cubic packing).

set of simultaneous equations for the parameters is obtained by requiring that the weighted average interior error for each of Equations (4) to (7) be zero for N different weight functions, over the region V. Here V is the fluid part of the region $0 < x^* < 1$, $0 < y^* < 1$, $0 < z^* < \sqrt{2}$. Galerkin's method requires that the weight functions be chosen from the trial function set; this requirement distinguishes the method from other weighted error methods (*11, 14*).

The choice of weight functions is restricted by the symmetry properties employed. Thus, when the function set is restricted by Equations (26) and (27), the errors ϵ_{vx}, ϵ_{vy}, and ϵ_{vz} in the equations of motion have the properties prescribed for the components of $\mathbf{v}^*$ in Equation (13), and the error ϵ_{vc} in the equation of continuity has the properties given for $\mathcal{P}_{per}^*$ in Equations (14) and (15). It follows that ϵ_{vx}, ϵ_{vy}, and ϵ_{vz} are already orthogonal to all of the functions ϕ_{Pj}, and ϵ_{vc} is already orthogonal to all the functions ϕ_{xj}, ϕ_{yj}, ϕ_{zj}, over the chosen region V. To determine the parameters it is necessary to impose additional orthogonality requirements; here ϕ_{zj} was used as weight for ϵ_{vx}, ϵ_{vy}, ϵ_{vz}, and

$$\phi'_{zj} = \cos\alpha'_j\, \pi x^* \cos\beta'_j\, \pi y^* \cos\gamma'_j \frac{\pi z^*}{\sqrt{2}} \qquad (28)$$

as weight for ϵ_{vc}. The set ϕ'_{zj} consists of the unused members of the set ϕ_{zj} of Equation (19), that is, those members that do not satisfy Equation (26). Several other choices of Galerkin weights are conceivable here but the above choice proved adequate.

The orthogonality relations thus obtained are as follows:

From the equation of continuity

$$\sum_{i=1}^{N} C_{xi} \int_V \int \int \left\{ \frac{\partial(\chi\phi_{xi})}{\partial x^*} \right\} \phi'_{zj} dV + \sum_{i=1}^{N} C_{yi} \int_V \int \int \left\{ \frac{\partial(\chi\phi_{yi})}{\partial y^*} \right\} \phi'_{zj} dV + \sum_{i=1}^{N} C_{zi} \int_V \int \int \left\{ \frac{\partial(\chi\phi_{zi})}{\partial z^*} \right\} \phi'_{zj}\, dV = 0$$
$$j = 1, 2, \ldots N \qquad (29)$$

From the x component of the equation of motion

$$\sum_{i=1}^{N} C_{xi} \int_V \int \int \{\nabla^2(\chi\phi_{xi})\}\, \phi_{zj} dV + \sum_{i=1}^{N} C_{Pi} \int_V \int \int \left\{ \frac{\partial\phi_{Pi}}{\partial x^*} \right\} \phi_{zj} dV = 0$$
$$j = 1, 2, \ldots N \qquad (30)$$

From the y component of the equation of motion

$$\sum_{i=1}^{N} C_{yi} \int_V \int \int \{\nabla^2(\chi\phi_{yi})\}\, \phi_{zj} dV + \sum_{i=1}^{N} C_{Pi} \int_V \int \int \left\{ \frac{\partial\phi_{Pi}}{\partial y^*} \right\} \phi_{zj} dV = 0$$
$$j = 1, 2, \ldots N \qquad (31)$$

And from the z component of the equation of motion

$$\sum_{i=1}^{N} C_{zi} \int_V \int \int \{\nabla^2(\chi\phi_{zi})\}\, \phi_{zj} dV + \sum_{i=1}^{N} C_{Pi} \int_V \int \int \left\{ \frac{\partial\phi_{Pi}}{\partial z^*} \right\} \phi_{zj} dV + \int_V \int \int \frac{\phi_{zj}}{2\sqrt{2}} dV = 0 \quad j = 1, 2, \ldots N \qquad (32)$$

This set of $4N$ linear algebraic equations was solved by a matrix inversion technique (*15*) to obtain the values of the trial function parameters.

The integrals in Equations (29) to (32) were evaluated numerically by triple Gaussian quadratures (*16*). The first solutions were obtained with five-point quadrature with respect to each coordinate; final results were obtained with higher order integrations. Previous experience indicated that significant errors could occur in such quadratures if any of the integration variables traversed a corner of the region V. Therefore, the quadratures were done separately over three subregions of V.

DISCUSSION OF THE APPROXIMATE SOLUTIONS

A number of approximate solutions were obtained in this study. Each solution was tested by calculating the dimensionless superficial velocity

$$v_o^* = \frac{1}{8\sqrt{2}} \int_{-\sqrt{2}}^{\sqrt{2}} \int_{-1}^{1} \int_{-1}^{1} v_z^*\, dx^* dy^* dz^* \qquad (33)$$

averaged over the unit cell. The averaging over z^* was done because the approximate solutions may deviate locally from Equation (4), and thus give slightly different volume flow rates at different cross sections. These predicted values of v_o^* were compared with Martin's experimental value (*1*) to estimate the accuracy of the predicted profiles.

The function χ_I was used in some preliminary calculations for small values of N. The predicted flow rates were less accurate than those obtained with χ_{II}, as expected. Addition of terms of higher degree in χ_I or χ_{II} was tested, but the addition of terms with higher trigonometric indices was found to give more rapid improvement.

After choosing the final form of the functions, we computed approximate solutions with N up to 30 with triple five-point Gaussian integration ($5^3 = 125$ points per subregion). The results for v_o^* vs. N (Figure 2) indicated that terms beyond $N = 22$ should be unimportant. Next, solutions with N up to 22 were computed with the Gaussian twelve-point formula ($12^3 = 1{,}728$ points per subregion) and the sixteen-point formula ($16^3 = 4{,}096$ points per subregion). The twelve- and sixteen-point formulas led to nearly identical profiles; the latter solutions are thus essentially free of truncation error in the integration. The predicted superficial velocities v_o^* are compared with an experimental value (*1*) in Figure 2.

Figure 2 shows that the predicted values of v_o^* are nearly independent of N beyond $N = 12$. The profiles

TABLE 1. SOLUTIONS FOR DENSE CUBIC PACKING

Trigonometric indices						Coefficients of the fourteen-term solution				Coefficients of the twenty-two-term solution			
i	α_i	β_i	γ_i	α'_i	β'_i	γ'_i	C_{xi}	C_{yi}	C_{zi}	C_{Pi}	C_{xi}	C_{yi}	C_{zi}	C_{Pi}
1	0	0	0	0	0	1	−0.24614	−0.24614	+0.83493	−0.01766	+2.97371	+2.97371	−19.01375	+0.47899
2	1	0	1	0	1	0	+0.69053	+1.04578	−0.66418	+0.05593	+4.29957	+7.06794	−43.61303	+0.68014
3	0	1	1	1	0	0	+1.04578	+0.69053	−0.66418	+0.05593	+7.06794	+4.29957	−43.61303	+0.68014
4	1	1	0	1	1	1	+1.46163	+1.46163	−0.70610	−0.04703	+6.44138	+6.44138	−37.99080	+0.84741
5	1	1	2	0	0	3	+0.62351	+0.62351	−0.79814	+0.02439	+3.21959	+3.21959	−27.59440	+0.07047
6	0	0	2	1	1	3	+0.28931	+0.28931	−1.33764	+0.03434	+2.97545	+2.97545	−15.79866	+0.09921
7	1	0	3	1	0	2	+0.38881	−0.24728	−1.03516	+0.01967	+0.64426	+1.06082	−5.22206	+0.34213
8	0	1	3	0	1	2	−0.24728	+0.38881	−1.03516	+0.01967	+1.06082	+0.64426	−5.22206	+0.34213
9	2	0	2	2	0	1	+0.46648	+0.02403	−0.19923	+0.01941	+0.67345	+1.21335	−5.63364	+0.20031
10	0	2	2	0	2	1	+0.02403	+0.46648	−0.19923	+0.01941	+1.21335	+0.67345	−5.63364	+0.20031
11	2	1	1	2	1	0	+0.84374	+0.01615	−0.25297	−0.00654	+2.53377	+1.94829	−16.27565	+0.20524
12	1	2	1	1	2	0	+0.01615	+0.84374	−0.25297	−0.00654	+1.94829	+2.53377	−16.27565	+0.20524
13	2	0	0	3	0	0	+0.17150	−0.34954	+0.12507	+0.00540	+1.45412	+1.32788	−7.75479	+0.00460
14	0	2	0	0	3	0	−0.34954	+0.17150	+0.12507	+0.00540	+1.32788	+1.45412	−7.75479	+0.00460
15	2	2	0	2	2	1					+0.53790	+0.53790	−2.47441	+0.03757
16	2	2	2	2	2	3					+0.21601	+0.21601	−1.46140	+0.01691
17	3	0	1	2	1	2					+0.00584	−0.05068	−0.42982	+0.10391
18	0	3	1	1	2	2					−0.05068	+0.00584	−0.42982	+0.10391
19	3	1	0	3	1	1					+0.15210	−0.03326	−0.29636	−0.00305
20	1	3	0	1	3	1					−0.03326	+0.15210	−0.29636	−0.00305
21	2	1	3	2	0	3					−0.10518	+0.10638	−1.45049	+0.01355
22	1	2	3	0	2	3					+0.10638	−0.10518	−1.45049	+0.01355

converge more slowly, as illustrated in Figure 3; the results for $N = 22$ are preferred. From comparisons of the trends with N in these two plots, the local values of v_z^* with $N = 22$ are estimated to be within about 10% of the true solution of the boundary value problem; this accuracy is adequate for the projected heat and mass transfer calculations.

RESULTS FOR DENSE CUBIC PACKING

The constants for the approximate solutions with $N = 14$ and $N = 22$ are presented in Table 1. Both sets of results are based on the highest order (sixteen-point) Gaussian integrations. One of the advantages in using a trial-function method is that the approximate solution is expressed in analytic form; thus extensive tabulation of the profiles is not necessary.

For illustration a few profiles calculated from the fourteen-term solution are shown here. Profiles of v_z^* at the cross sections $z^* = \sqrt{2}$ and $z^* = \sqrt{2}/2$ are shown in Figures 4 and 5. The lines of constant v_z^* are shaped much like the lines of constant χ_{II}. At $z^* = \sqrt{2}$, v_x^* and v_y^* are zero, and $\mathcal{P}^*$ is unity over the entire cross section. The profiles of v_z^* and $\mathcal{P}^*$ at $z^* = \sqrt{2}/2$ are shown in Figures 6 and 7, respectively. It can be seen that $\mathcal{P}_{per}^*$ is not large, since the nonperiodic pressure term $(z^* + \sqrt{2})/2\sqrt{2}$ is 0.75 at this cross section. The profiles from the twenty-two-term solution would have somewhat different values, but the shapes of the contours would be quite similar.

The predicted relationship between pressure drop and flow rate is contained in the dimensionless superficial velocity v_0^*. From the solutions with large N, the extrapolated value $v_0^* = 0.000258$ was obtained. This gives the predicted friction factor relationship

$$f = \frac{(\mathcal{P}_0 - \mathcal{P}_L)\rho}{G_0^2}\,\frac{D_p}{L}\,\frac{\epsilon^3}{1-\epsilon} = 175\left(\frac{D_p G_0}{\mu(1-\epsilon)}\right)^{-1} = 175\,N_{Re}^{-1} \qquad (35)$$

This result is compared in Figure 8 with data and other predictions. For a given pressure drop, the superficial velocity predicted by this investigation is 4.4% lower than the experimental data (*1*), 3.5% higher than the Carman correlation (*3*), 13.6% lower than the Blake-Kozeny correlation (*2*), and 9.1% lower than the predicted value of Happel (*5*). Experimental measurements indicate that the creeping flow region extends up to approximately $N_{Re} = 20$ in this flow geometry.

EXTENSION TO OTHER REGULAR PACKING ARRANGEMENTS

The method of solution given above is adaptable to beds of spheres in other regular arrangements. The problem statement and trial functions have to be rewritten, of

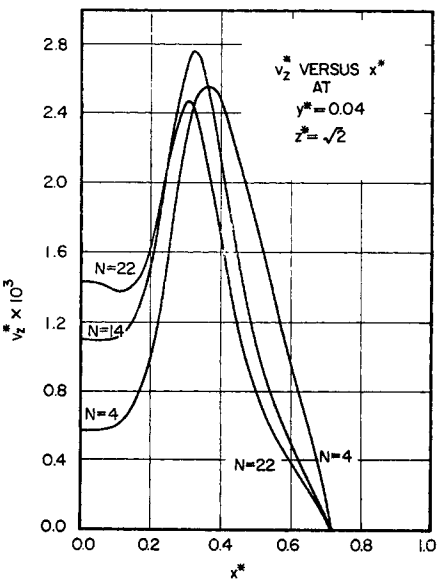

Fig. 3. Comparison of velocity profiles from the four-, fourteen-, and twenty-two-term approximate solutions (dense cubic packing).

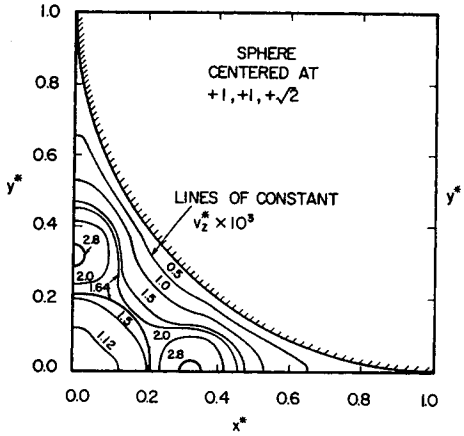

Fig. 4. Profiles of v_z^* at $z^* = \sqrt{2}$ (dense cubic packing).

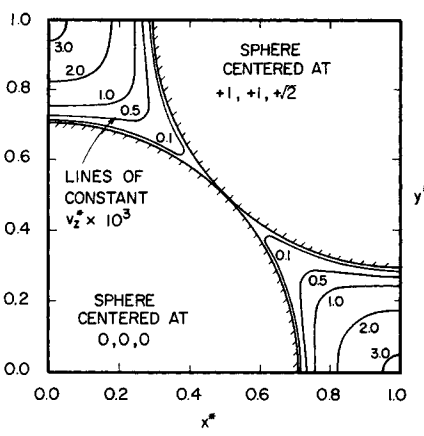

Fig. 5. Profiles of v_z^* at $z^* = \sqrt{2}/2$ (dense cubic packing).

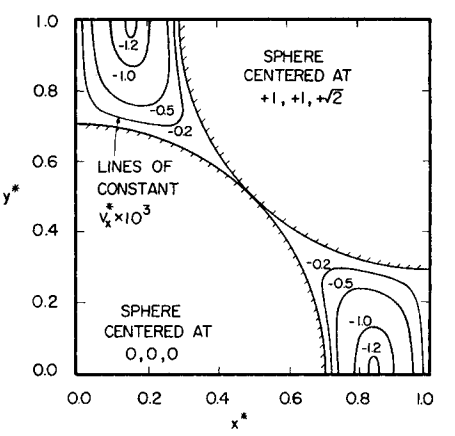

Fig. 6. Profiles of v_x^* at $z^* = \sqrt{2}/2$ (dense cubic packing).

course, for the arrangement in question. Velocity and pressure profiles were obtained for flow through a bed of spheres in simple cubic packing by introducing the following three modifications: (1) The length L of the unit cell becomes $2R$ rather than $2\sqrt{2}R$; therefore, in Equations (1) to (12) and (16) to (33), $\sqrt{2}$ is replaced by unity. (2) Equations (13), (14), and (15) are changed by substitution of 2 for each of the symbols 1, $\sqrt{2}$, and $2\sqrt{2}$; Equations (26) and (27) then are dropped, and the function ϕ'_{zj} may be replaced by ϕ_{zj}. (3) The sphere coordinates x_i^*, y_i^*, z_i^* are changed to represent simple cubic packing.

Approximate solutions with $N \leq 28$ were obtained with the twelve-point Gaussian quadrature formula. The constants of the twenty-eight-term solution are given in Table 2. The superficial velocity v_0^* predicted by solutions with $19 \leq N \leq 28$ was 0.00525 ± 0.00008; this leads to the friction factor relation

$$f = \frac{(\mathcal{P}_0 - \mathcal{P}_L)\rho}{G_0^2} \frac{D_p}{L} \frac{\epsilon^3}{1-\epsilon} = 150 \left(\frac{D_p G_0}{\mu(1-\epsilon)}\right)^{-1} = 150\, N_{Re}^{-1} \qquad (36)$$

which is plotted in Figure 9. The flow rate predicted by this equation is within 5% of Martin's experimental data (*1*) and only 0.5% higher than the Blake-Kozeny correlation (*2*).

SUMMARY

Velocity and pressure profiles were calculated by Galerkin's method for Newtonian creeping flow through dense cubic and simple cubic beds of spheres. The pres-

TABLE 2. TRIGONOMETRIC INDICES AND COEFFICIENTS OF THE TWENTY-EIGHT-TERM SOLUTION, SIMPLE CUBIC PACKING*

i	α_i	β_i	γ_i	α'_i	β'_i	γ'_i	C_{xi}	C_{yi}	C_{zi}	C_{Pi}
1	0	0	0	0	0	0	+0.21068	+0.21068	−10.95001	+3.29994
2	0	1	0	0	1	0	−0.50845	−0.08177	+15.62258	−4.70731
3	1	0	0	1	0	0	−0.08177	−0.50845	+15.62258	−4.70731
4	0	0	1	0	0	1	−0.23887	−0.23887	+13.90695	−3.36025
5	1	0	1	1	0	1	−0.09067	+0.43704	−19.26880	+4.51965
6	0	1	1	0	1	1	+0.43704	−0.09067	−19.26880	+4.51965
7	1	1	0	1	1	0	+0.04767	+0.04767	−19.90245	+6.25696
8	1	1	1	1	1	1	+0.16389	+0.16389	+24.03481	−5.83870
9	2	0	0	2	0	0	+0.02146	+0.09674	−3.96945	+1.22007
10	0	2	0	0	2	0	+0.09674	+0.02146	−3.96945	+1.22007
11	0	0	2	0	0	2	+0.17656	+0.17656	−2.84983	+0.99155
12	2	1	0	2	1	0	+0.00868	+0.04696	+4.94766	−1.47097
13	1	2	0	1	2	0	+0.04696	+0.00868	+4.94766	−1.47097
14	2	0	1	2	0	1	+0.08476	−0.10784	+4.50395	−1.08164
15	0	2	1	0	2	1	−0.10784	+0.08476	+4.50395	−1.08164
16	1	0	2	1	0	2	+0.12141	+0.00411	+3.75407	−1.59134
17	0	1	2	0	1	2	+0.12141	+0.12141	+3.75407	−1.59134
18	2	1	1	2	1	1	−0.07755	−0.13420	−5.66428	+1.22432
19	1	2	1	1	2	1	−0.13420	−0.07755	−5.66428	+1.22432
20	1	1	2	1	1	2	−0.23781	−0.23781	−4.14314	+1.63530
21	2	2	0	2	2	0	+0.02849	+0.02849	−0.58793	+0.22929
22	2	0	2	2	0	2	−0.02805	+0.05731	−0.52553	+0.25345
23	0	2	2	0	2	2	+0.05731	−0.02805	−0.52553	+0.25345
24	2	2	1	2	2	1	−0.00631	−0.00631	+0.37583	−0.15442
25	2	1	2	2	1	2	+0.01642	+0.05532	+0.55159	−0.29165
26	1	2	2	1	2	2	+0.05532	+0.01642	+0.55159	−0.29165
27	0	3	0	0	3	0	+0.03055	−0.02083	+0.12385	−0.02953
28	3	0	0	3	0	0	−0.02083	+0.03055	+0.12385	−0.02953

* To be used in Equations (19) to (22) with $\sqrt{2}$ replaced by unity and with L and χ_{II} evaluation for simple cubic packing.

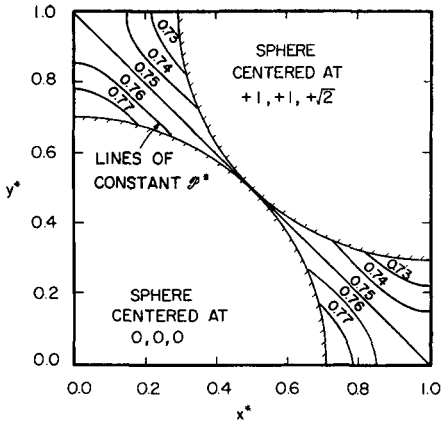

Fig. 7. Profiles of $\mathcal{P}^*$ at $z^* = \sqrt{2}/2$ (dense cubic packing).

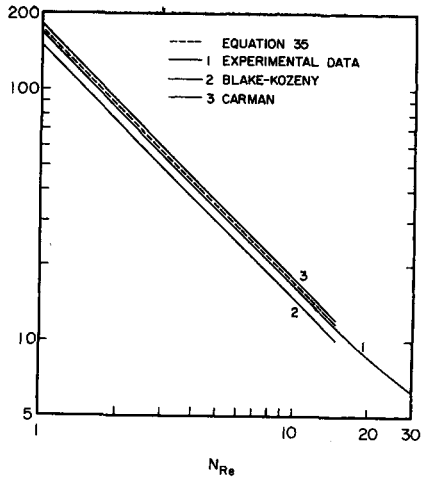

Fig. 8. Friction factors for dense cubic packing.

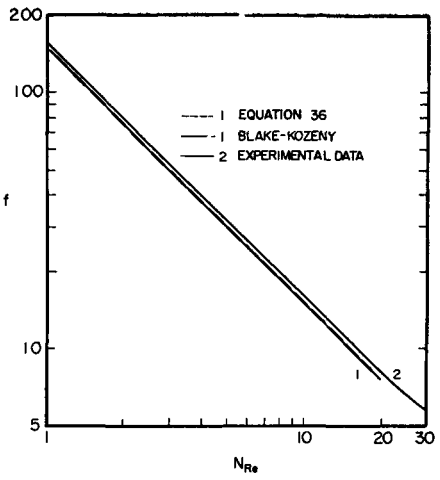

Fig. 9. Friction factors for simple cubic packing.

sure drop relationships obtained from these calculations are within 5% of experimental values. The profiles are currently being used in a theoretical investigation of heat and mass transfer in these systems.

A number of the advantages of Galerkin's method are demonstrated by these results. This approach to the numerical solution of boundary value problems should be useful in many engineering applications.

ACKNOWLEDGMENT

The authors wish to thank the Wisconsin Alumni Research Foundation and the National Science Foundation for supporting the computational program, and the University of Wisconsin Computing Center for the use of their facilities. In addition, one of us (L.J.S.) received fellowship support from the Wisconsin Alumni Research Foundation and the other (W.E.S.) received summer salary from National Science Foundation Grant G-14812.

It is also a pleasure to acknowledge helpful discussions with Dr. Howard Brenner and Dr. Millard Johnson.

NOTATION

C_{xi} = coefficients in Equation (20)
C_{yi} = coefficients in Equation (21)
C_{zi} = coefficients in Equation (19)
C_{Pi} = coefficients in Equation (22)
D_p = $2R$, diameter of the spheres in the packed bed
f = friction factor
G_0 = ρv_0, superficial mass velocity
g = acceleration of gravity
h = elevation above potential energy datum
L = distance used in defining $(\mathcal{P}_0 - \mathcal{P}_L)$. For dense cubic packing $L = 2\sqrt{2}R$; for simple cubic packing $L = 2R$
N = number of terms in an approximate solution
N_{Re} = $D_p G_0/\mu(1-\epsilon)$, Reynolds number
$\mathcal{P}$ = $p + \rho gh$, pressure function
$\mathcal{P}^*$ = dimensionless pressure function
$(\mathcal{P}_0 - \mathcal{P}_L)$ = characteristic pressure drop
$\mathcal{P}_{per}^*$ = $\mathcal{P}^* - (z^* + \sqrt{2})/2\sqrt{2}$, the periodic portion of the pressure function
R = radius of the spheres in the packed bed
V = fluid part of the region $x^* > 0$, $y^* > 0$, $z^* > 0$ in the unit cell
$\mathbf{v}$ = velocity vector
$\mathbf{v}^*$ = dimensionless velocity vector; see Equation (2)
v_x^*, v_y^*, v_z^* = dimensionless velocity components
v_0 = superficial velocity
v_0^* = dimensionless superficial velocity
x, y, z = rectangular coordinates
x^*, y^*, z^* = dimensionless rectangular coordinates; see Equation (1)
x_l^*, y_l^*, z_l^* = dimensionless coordinates of the center of the l^{th} sphere

Greek Letters

$\alpha_i, \beta_i, \gamma_i, \alpha_i', \beta_i', \gamma_i'$ = trigonometric indices in Equations (19) to (22)
ϵ = void fraction external to the particles in the packed bed
ϵ_V = the interior error; the amount by which the approximate solution fails to satisfy a differential equation within V
μ = fluid viscosity
ρ = fluid density
χ = an arbitrary no-slip function
χ_I = the no-slip function defined by Equation (24)
χ_{II} = the no-slip function defined by Equation (25)

Subscripts

i = term number in the trial solutions
j = weighting function number in Equations (28) to (32)

LITERATURE CITED

1. Martin, J. J., W. L. McCabe, and C. C. Monrad, *Chem. Eng. Progr.*, **47**, 91 (1951).
2. Bird, R. B., W. E. Stewart, and E. N. Lightfoot, "Transport Phenomena," p. 196, Wiley, New York (1960).
3. Carman, P. C., *Trans. Inst. Chem. Engrs. (London)*, **15**, 150 (1937).
4. Ranz, W. E., *Chem. Eng. Progr.*, **48**, 247 (1952).
5. Happel, John, *A.I.Ch.E. J.* **4**, No. 2, 197 (1958).
6. Uchida, S., *Rept. Inst. Sci. Technol. Tokyo*, **3**, 97 (1949); abstracted in *Ind. Eng. Chem.*, **46**, 1194 (1954).
7. Brenner, Howard, Sc.D. thesis, New York Univ., New York (1957).
8. Hasimoto, H., *J. Fluid Mech.*, **5**, 317 (1959).
9. Johnson, M. W., Jr., *Phys. Fluids*, **3**, 871 (1960).
10. Snyder, L. J., T. W. Spriggs, and W. E. Stewart, *A.I.Ch.E. J.*, **10**, 535 (1964).
11. B. A. Finlayson, and L. E. Scriven, *Chem. Eng. Sci.*, **20**, 395 (1965).
12. Courant, R., and D. Hilbert, "Methods of Mathematical Physics," Vol. I, Interscience, New York (1953).
13. Snyder, L. J., Ph.D. Thesis, Univ. Wisconsin, Madison (1965).
14. Crandall, S. H., "Engineering Analysis," McGraw-Hill, New York (1956).
15. Fadeeva, V. N., "Computational Methods of Linear Algebra," p. 85, Dover, New York (1959).
16. Krylov, V. I., "Approximate Calculation of Integrals," Macmillan, New York (1962).

Manuscript received March 9, 1965; revision received September 9, 1965; paper accepted March 10, 1965. Paper presented at A.I.Ch.E. Houston meeting.